Published in final edited form as:
Nature. 2012 May 10; 485(7397): 251–255. doi:10.1038/nature10992.

Mitochondrial DNA That Escapes from Autophagy Causes Inflammation and Heart Failure

Takafumi Oka[1], **Shungo Hikoso**[1], **Osamu Yamaguchi**[1], **Manabu Taneike**[1,2], **Toshihiro Takeda**[1], **Takahito Tamai**[1], **Jota Oyabu**[1], **Tomokazu Murakawa**[1], **Hiroyuki Nakayama**[3], **Kazuhiko Nishida**[1,2], **Shizuo Akira**[4,5], **Akitsugu Yamamoto**[6], **Issei Komuro**[1], and **Kinya Otsu**[1,2]

[1]Department of Cardiovascular Medicine, Osaka University Graduate School of Medicine, Suita, Osaka 565-0871, Japan

[2]Cardiovascular Division, King's College London, London SE5 9NU, UK

[3]Department of Clinical Pharmacology and Pharmacogenomics, Graduate School of Pharmaceutical Sciences, Osaka University, Suita, Osaka 565-0871

[4]Laboratory of Host Defense, WPI Immunology Frontier Research Center, Osaka University, Suita, Osaka 565-0871

[5]Department of Host Defense, Research Institute for Microbial Diseases, Osaka University, Suita, Osaka 565-0871

[6]Faculty of Bioscience, Nagahama Institute of Bio-Science and Technology, Nagahama, Shiga 526-0829, Japan

Abstract

Heart failure is a leading cause of morbidity and mortality in industrialized countries. Although infection with microorganisms is not involved in the development of heart failure in most cases, inflammation has been implicated in the pathogenesis of heart failure[1]. However, the mechanisms responsible for initiating and integrating inflammatory responses within the heart remain poorly defined. Mitochondria are evolutionary endosymbionts derived from bacteria and contain DNA similar to bacterial DNA[2,3,4]. Mitochondria damaged by external hemodynamic stress are degraded by the autophagy/lysosome system in cardiomyocytes[5]. Here, we show that mitochondrial DNA that escapes from autophagy cell-autonomously leads to Toll-like receptor (TLR) 9-mediated inflammatory responses in cardiomyocytes and is capable of inducing myocarditis, and dilated cardiomyopathy. Cardiac-specific deletion of lysosomal deoxyribonuclease (DNase) II showed no cardiac phenotypes under baseline conditions, but increased mortality and caused severe myocarditis and dilated cardiomyopathy 10 days after treatment with pressure overload. Early in the pathogenesis, DNase II-deficient hearts exhibited infiltration of inflammatory cells and increased mRNA expression of inflammatory cytokines, with accumulation of mitochondrial DNA deposits in autolysosomes in the myocardium. Administration of the inhibitory oligodeoxynucleotides against TLR9, which is known to be

Correspondence should be addressed to Kinya Otsu, Cardiovascular Division, King's College London, The James Black Centre, 125 Coldharbour Lane, London SE5 9NU, UK. Tel: 44-20-7848-5128, Fax: 44-20-7848-5193, kinya.otsu@kcl.ac.uk..

Author Contributions

A.S. and I.K. provided essential intellectual input; K.O. was responsible for the overall study design and for writing the manuscript and the remaining authors performed experiments and analyzed data.
All authors contributed to the discussions.

Competing financial interests

The authors declare no competing financial interests.

Europe PMC Funders Author Manuscripts

activated by bacterial DNA[6], or ablation of *Tlr9* attenuated the development of cardiomyopathy in DNase II-deficient mice. Furthermore, *Tlr9*-ablation improved pressure overload-induced cardiac dysfunction and inflammation even in mice with wild-type *Dnase2a* alleles. These data provide new perspectives on the mechanism of genesis of chronic inflammation in failing hearts.

Mitochondrial DNA has similarities to bacterial DNA, which contains inflammatogenic unmethylated CpG motifs[2,3,4,7,8]. Damaged mitochondria are degraded by autophagy, which involves the sequestration of cytoplasmic contents in a double-membraned vacuole, the autophagosome and the fusion of the autophagosome with the lysosome[9]. Pressure overload induces the impairment of mitochondrial cristae morphology and functions in the heart[10,11]. We have previously reported that autophagy is an adaptive mechanism to protect the heart from hemodynamic stress[5].

DNase II, encoded by *Dnase2a*, is an acid DNase found in the lysosome[12]. DNase II in macrophages has an essential role in the degradation of the DNA of apoptotic cells after macrophages engulf them[13]. In the present study, we hypothesized that DNase II in cardiomyocytes digests mitochondrial DNA in the autophagy system to protect the heart from inflammation in response to hemodynamic stress.

First, we examined the alteration of DNase II activity in the heart in response to pressure overload. In wild-type mice, pressure overload by thoracic transverse aortic constriction (TAC) induced cardiac hypertrophy 1 week after TAC and heart failure 8-10 weeks after TAC[5]. DNase II activity was upregulated in hypertrophied hearts, but not in failing hearts (Supplementary Fig. 1a). Immunohistochemical analysis showed infiltration of $CD45^+$ leukocytes, including $CD68^+$ macrophages in failing hearts (Supplementary Fig. 1b). Then, we stained the heart sections with PicoGreen[14], anti-LAMP2a and anti-LC3[15] antibodies, which was used for the detection of DNA, lysosomes, and autophagosomes, respectively (Supplementary Fig. 1c, d and 2a). We observed PicoGreen- and LAMP2a-positive deposits and PicoGreen- and LC3-positive deposits in failing hearts, but not in hypertrophied hearts, suggesting the accumulation of DNA in autolysosomes in failing hearts.

We crossed mice bearing a $Dnase2a^{flox}$ allele[13] with transgenic mice expressing *Cre* recombinase under the control of the α-myosin heavy chain promoter (α-MyHC)[16], to produce $Dnase2a^{flox/flox}$;α-MyHC-Cre^+ ($Dnase2a^{-/-}$) mice. We used $Dnase2a^{flox/flox}$;α-MyHC-Cre^- littermates ($Dnase2a^{+/+}$) as controls. The resulting $Dnase2a^{-/-}$ mice were born at the expected Mendelian frequency. In $Dnase2a^{-/-}$ mice, we observed 90.1% reduction in the level of *Dnase2a* mRNA and 95.1% decrease in DNase II activity in purified adult cardiomyocyte preparation (Supplementary Fig. 3a, b). Physiological parameters and basal cardiac function assessed by echocardiography showed no differences between $Dnase2a^{+/+}$ and $Dnase2a^{-/-}$ mice (Supplementary Table 1). These results indicate that DNase II does not appear to be required during normal embryonic development or for normal heart growth in the postnatal period.

To clarify the role of DNase II in cardiac remodeling, $Dnase2a^{-/-}$ mice were subjected to TAC. DNase II activity was upregulated in response to pressure overload in $Dnase2a^{+/+}$ hearts and was lower in sham- and TAC-operated $Dnase2a^{-/-}$ hearts than that in the corresponding controls (Supplementary Fig. 3c). Twenty-eight days after TAC, 57.1% of $Dnase2a^{-/-}$ mice had died, whereas 85.7% of $Dnase2a^{+/+}$ mice were still alive (Fig. 1a). The $Dnase2a^{-/-}$ hearts exhibited left ventricular dilatation and severe contractile dysfunction 10 days after TAC (Fig. 1b, c, d, Supplementary Table 2). The lung-to-body weight ratio, an index of lung congestion, was elevated in TAC-operated $Dnase2a^{-/-}$ mice (Fig. 1e). The increases in the heart-to-body weight ratio and cardiomyocyte cross-sectional area by TAC were larger in $Dnase2a^{-/-}$ mice than in $Dnase2a^{+/+}$ mice (Fig. 1e, f). TAC-operated

Dnase2a$^{-/-}$ hearts exhibited massive cell infiltration, (Fig. 1f). Immunohistochemical analysis of the hearts showed infiltration of CD45^{+} leukocytes, including CD68^{+} macrophages (Supplementary Fig. 4a). The mRNA level of interleukin (IL)-6 (*Il6*) was upregulated, but not other cytokine mRNAs in TAC-operated *Dnase2a*$^{-/-}$ hearts (Supplementary Fig. 4b). TAC-operated *Dnase2a*$^{-/-}$ hearts exhibited intermuscular and perivascular fibrosis with increased mRNA expression of α2 Type I collagen (*Col1a2*) (Fig. 1g, Supplementary Fig. 3d). Ultrastructural analysis of TAC-operated *Dnase2a*$^{-/-}$ hearts showed a disorganized sarcomere structure, misalignment and aggregation of mitochondria, and aberrant electron-dense structures (Supplementary Fig. 4c). The mRNA levels of atrial natriuretic factor (*Nppa*) and brain natriuretic peptide (*Nppb*) were higher in TAC-operated *Dnase2a*$^{-/-}$ mice than in TAC-operated *Dnase2a*$^{+/+}$ mice (Supplementary Fig. 3d). These data suggest that DNase II plays an important role in preventing pressure overload-induced heart failure and myocarditis.

To clarify the molecular mechanisms underlying the cardiac abnormalities observed in *Dnase2a*$^{-/-}$ mice, we evaluated the phenotypes in the earlier time course after pressure overload. Chamber dilation and cardiac dysfunction developed with time after TAC in *Dnase2a*$^{-/-}$ mice (Supplementary Fig. 5a). We chose to perform the analysis 2 days after TAC to minimize the contributions of operation-related events and phenomena secondary to the initial and essential molecular event that induced cardiomyopathy. TAC-operated *Dnase2a*$^{-/-}$ hearts exhibited cell infiltration without apparent fibrosis (Fig. 2a, b) and infiltration of CD68^{+} macrophages and Ly6G^{+} cells (Fig. 2c). We detected increases in the mRNA levels of IL-1β (*Il1b*) and *Il6*, but not interferon β (*Ifnb1*) and γ (*Ifng*) or TNFα in TAC-operated *Dnase2a*$^{-/-}$ hearts (Supplementary Fig. 6a). In order to identify the source of IL-1β and IL-6, we performed *in situ* hybridization analysis in heart sections. *Il1b* and *Il6* mRNA-positive cardiomyocytes were evident in TAC-operated *Dnase2a*$^{-/-}$ hearts (Supplementary Fig. 4d).

Ultrastructural analysis exhibited aberrant electron-dense deposits without apparent changes in sarcomeric and mitochondrial structures in TAC-operated *Dnase2a*$^{-/-}$ hearts (Fig. 3a). At higher magnification, the electron-dense deposits appeared to be autolysosomes (Fig. 3a). Immunoelectron microscopic analysis using anti-DNA antibody exhibited DNA deposition in autolysosomes (Fig. 3b). In TAC-operated *Dnase2a*$^{-/-}$ hearts, we observed PicoGreen- and LAMP2a-positive deposits and PicoGreen- and LC3-positive deposits (Supplementary Fig. 6b, c, 2b). The PicoGreen-positive deposits were not TUNEL-positive (Supplementary Fig. 6d), indicating that the DNA was not derived from fragmented nuclear DNA. To label mitochondrial DNA, mice were injected with EdU (5-ethynyl-2′-deoxyuridine) 5 times before TAC. EdU, a nucleoside analog to thymidine, is incorporated into DNA during active DNA synthesis[17]. EdU specifically binds to mitochondrial DNA during its active DNA synthesis in non-dividing cardiomyocytes. In TAC-operated *Dnase2a*$^{-/-}$ hearts, we observed EdU- and LAMP2a-positive deposits and EdU- and LC3-positive deposits (Fig. 3c, d, Supplementary Fig. 2c), indicating that mitochondrial DNA accumulated in autolysosomes.

The innate immune system is the major contributor to acute inflammation induced by microbial infection[18]. TLR9, localized in the endolysosome, senses DNA with unmethylated CpG motifs derived from bacteria and viruses. Mitochondrial DNA activates polymorphonuclear neutrophils through CpG/TLR9 interactions[19]. Immunohistochemical analysis indicated that TLR9 was colocalized with EdU-positive deposits (Fig. 3e). TLR9 is activated by synthetic oligodeoxynucleotides (ODN1668) that contain unmethylatedCpG[6], but it is inhibited by inhibitory ligands, such as ODN2088[20], in which “gcgtt” in ODN1668 is replaced with “gcggg”. ODN1668 induced increases in *Il1b* and *Il6* mRNA levels in wild-type isolated adult cardiomyocytes (data not shown). We, then, examined the effect of ODN2088 on carbonyl cyanide *m*-chlorophenyl hydrazone (CCCP) or isoproterenol-induced

cell death using isolated adult cardiomyocytes to eliminate the contribution of immune cells[5]. CCCP, a protonophore, induces dissipation of mitochondrial membrane potential. Isoproterenol caused a loss of mitochondrial membrane potential in wild-type cardiomyocytes, as indicated by loss of tetramethylrhodamine ethyl ester (TMRE) signal (Supplementary Fig. 7a). Incubation with CCCP or isoproterenol induced conversion of LC3-I to LC3-II, an essential step during autophagosome formation and treatment with the lysosomal inhibitor bafilomycin A1 led to an even larger increase of LC3-II in CCCP or isoproterenol-treated cells than in control cells, indicating that CCCP or isoproterenol accelerated autophagic flux (Supplementary Fig. 7b). Isolated cardiomyocytes from *Dnase2a*$^{-/-}$ hearts were more susceptible than those from control hearts to CCCP or isoproterenol in the presence of inactive control oligodeoxynucleotides (ODN2088 control) (Supplementary Fig. 7c, d, e). CCCP upregulated the mRNA expression levels of *Il1b* and *Il6* in *Dnase2a*$^{-/-}$ cardiomyocytes (Supplementary Fig. 7f). Incubation of *Dnase2a*$^{-/-}$ cardiomyocytes with ODN2088 attenuated the cell death and cytokine mRNA induction by CCCP treatment. Treatment of the *Dnase2a*$^{-/-}$ cardiomyocytes with 3-methyladenine, an autophagy inhibitor and rapamycin, an autophagy inducer, inhibited and enhanced the induction of the cytokine mRNA by CCCP treatment, respectively (Supplementary Fig. 7g).

We next examined whether the inhibition of TLR9 can rescue the cardiac phenotypes in TAC-operated *Dnase2a*$^{-/-}$ mice. Administration of ODN2088 resulted in the improvement of survival 28 days after TAC (Fig. 4a). ODN2088 attenuated chamber dilation and cardiac dysfunction compared to the control oligodeoxynucleotides 4 days after TAC (Fig. 4b, c, Supplementary Fig. 8a). In addition, ODN2088 inhibited infiltration of CD68^{+} macrophages and Ly6G^{+} cells, fibrosis and upregulation of *Il6*, *Ifng*, *Nppa* and *Col1a2* mRNAs in TAC-operated *Dnase2a*$^{-/-}$ hearts (Fig. 4d, Supplementary Fig. 8b, c, d, e). ODN2088 prevented cardiac remodeling for a longer time period (LVIDd (mm), 2.74 ± 0.03, 2.76 ± 0.03; LVIDs (mm), 1.37 ± 0.03, 1.34 ± 0.05; LVFS (%), 50.1 ± 0.7, 51.4 ± 1.5, before and 14 days after TAC, respectively, n = 6). Furthermore, ablation of *Tlr9* rescued the cardiac phenotypes in TAC-operated *Dnase2a*$^{-/-}$ mice (Supplementary Fig. 9).

To examine the significance of TLR9 signaling pathway in the genesis of heart failure, we subjected TLR9-deficient mice[6] to TAC. Ten weeks after TAC, TLR9-deficient mice showed smaller left ventricular dimensions, better cardiac function and less pulmonary congestion than in TAC-operated control mice (Fig. 4e, f, Supplementary Fig. 10a). The extent of fibrosis, the levels of *Nppa*, *Nppb* and *Col1a2* mRNA, infiltration of CD68^{+} macrophages were attenuated in TLR9-deficient mice (Supplementary Fig. 10b, c, d, e). We detected no significant differences in the cytokine mRNA levels between TAC-operated groups (Supplementary Fig. 10f). Furthermore, ODN2088 improved survival of wild-type mice in a more severe TAC model (Supplementary Fig. 10g). These data indicate that the TLR9 signaling pathway is involved in inflammatory responses in failing hearts in response to pressure overload and plays an important role in the pathogenesis of heart failure.

In this study, we showed that mitochondrial DNA that escapes from autophagy-mediated degradation cell-autonomously leads to TLR9-mediated inflammatory responses in cardiomyocytes, myocarditis, and dilated cardiomyopathy. Immune responses are initiated and perpetuated by endogenous molecules released from necrotic cells, in addition to pathogen-associated molecular patterns molecules expressed in invading microorganisms[21]. Cellular disruption by trauma releases mitochondrial molecules including DNA into circulation to cause systemic inflammation[19]. Depletion of autophagic proteins promotes cytosolic translocation of mitochondrial DNA and caspase-1-dependent cytokines mediated by the NALP3 inflammasome in response to lipopolysaccharide in macrophages[22]. We observed no significant difference in the amount of mitochondrial DNA in the blood between TAC-operated *Dnase2a*$^{-/-}$ and *Dnase2a*$^{+/+}$ mice (data not shown), excluding a

possibility that circulating mitochondrial DNA is causing the majority of the inflammatory responses mediated by TLR9. The mechanisms presented here do not require release of mitochondrial DNA from cardiomyocytes into extracellular space.

Increased levels of circulating proinflammatory cytokines are associated with disease progression and adverse outcomes in chronic heart failure patients[1]. Mitochondrial DNA plays an important role in inducing and maintaining inflammation in the heart. This mechanism might work in many chronic non-infectious inflammation-related diseases such as atherosclerosis, metabolic syndrome and diabetes mellitus.

Methods Summary

Animal study

The study was carried out under the supervision of the Animal Research Committee of Osaka University and in accordance with the Japanese Act on Welfare and Management of Animals (No. 105). The 12-14-week-old mice were subjected to TAC[5,23] and severe TAC using 26 and 27 G needles for aortic constriction, respectively.

Biochemical assays

The DNase II activity was determined using the single radial enzyme-diffusion (SRED) method[24]. The mRNA levels were determined by quantitative RT-PCR[5].

Histological Analysis

The antibodies used were anti-mouse CD45 (ANASPEC), CD68 (Serotec), Ly6G/6C (BD Pharmingen), CD3 (Abcam), DNA (Abcam), LAMP2a (Zymed), LC3[25], and TLR9 (Santa-Cruz). The *in situ* hybridization analysis was performed using DIG RNA Labeling Kit and DIG Nucleic Acid Detection Kit (Roche Diagnostics). Hearts were embedded in the LR White resin for immunoelectron microscopy[26]. Heart sections were incubated in PicoGreen (Molecular Probes) for 1 hour. Twenty-four hours before TAC, mice were injected i.p. with 250 μg of EdU every 2 hours 5 times and EdU was detected using Click-iT EdU Alexa Fluor 488 Imaging Kit (Invitrogen).

In vitro and in vivo rescue experiments with the TLR9 inhibitor

Cardiomyocytes[5] were pretreated with 1 μg/ml inhibitory CpG (ODN2088) or control (ODN2088 control) oligodeoxynucleotides for 5 hours and incubated with 20 nM CCCP or 50 μM isoproterenol for 24 hours[20]. The cells were loaded with TMRE (Molecular Probe) at 10 nM for 30 minutes. The mice were injected i.v. with 500 μg of the oligodeoxynucleotides 2 hours before and 2 and 4 days after TAC and every 3 days thereafter.

Statistical analysis

Results are shown as the mean ± s.e.m. Paired data were evaluated using a Student's t-test. A 1-way ANOVA with the Bonferroni post hoc test was used for multiple comparisons. The Kaplan-Meier method with a Logrank test was used for survival analysis.

Supplementary Material

Refer to Web version on PubMed Central for supplementary material.

Acknowledgments

We would like to thank Prof. Shigekazu Nagata and Dr. Kohki Kawane, Kyoto University, for valuable discussions and a generous gift of *Dnase2a*$^{flox/flox}$ mice and Prof. Yasuo Uchiyama, Juntendo University, for anti-LC3

antibody. We also thank Ms. Kana Takada for technical assistance. This work was supported by a Grant-in-Aid for Scientific Research from the Ministry of Education, Culture, Sports, Science and Technology in Japan and research grants from Mitsubishi Pharma Research Foundation and the British Heart Foundation (CH/11/3/29051, RG/11/12/29052).

Appendix

Methods

Animal study

The study was carried out under the supervision of the Animal Research Committee of Osaka University and in accordance with the Japanese Act on Welfare and Management of Animals (No. 105).

We crossed mice bearing a *Dnase2a*^{flox} allele[13] with transgenic mice expressing *Cre* recombinase under the control of the α-myosin heavy chain promoter (α-MyHC)[16], to produce cardiac-specific DNase II-deficient mice, *Dnase2a*$^{flox/flox}$;α-MyHC-*Cre*$^{+}$ (*Dnase2a*$^{-/-}$). To generate double knockout mice of *Dnase2a* and *Tlr9*, we crossed *Dnase2a*$^{-/-}$ mice with *Tlr9*$^{-/-}$ mice[6].

The 12-14-week-old male mice were subjected to TAC[5,23] and severe TAC using 26 and 27 G needles for aortic constriction, respectively. Noninvasive measurements of blood pressure were carried out on mice anesthetized with 2.5% avertin using a BP Monitor for Rats and Mice Model MK-2000 (Muromachi Kikai, Tokyo, Japan) according to the instructions of the manufacturer[5,23]. To perform echocardiography on awakened mice, ultra-sonography (SONOS-5500, equipped with a 15-MHz linear transducer, Philips Medical Systems) was used. The heart was imaged in the two-dimensional parasternal short-axis view, and an M-mode echocardiogram of the midventricle was recorded at the level of the papillary muscles. Heart rate, intra-ventricular septum and posterior wall thickness, and end-diastolic and end-systolic internal dimensions of the LV were obtained from the M-mode image.

Measurement of DNase II activity

The DNase II activity was determined using the single radial enzyme-diffusion (SRED) method[24]. The heart homogenates were applied to the cylindrical wells (radius, 1.5 mm) punched in 1% (w/v) agarose gel, containing 0.05 mg/ml salmon sperm DNA (Type III), 5 μg/ml ethidium bromide, 0.5 M sodium acetate buffer (pH 4.7) and 10 mM EDTA. After incubation for 48 hours at 37°C, the radius of the dark circle was measured under an UV transilluminator at 312 nm. DNase II activities for the samples were determined using a standard curve constructed from the serial dilution of porcine DNase II (Sigma).

Quantitative RT-PCR

Total RNA was isolated from the left ventricle or cultured cardiomyocytes for analysis using the TRIzol reagent (Invitrogen Life Technologies). The mRNA levels were determined by quantitative RT-PCR[5]. For reverse transcription and amplification, we used the TaqMan Reverse Transcription Reagents (Applied Biosystems) and Platinum Quantitative PCR SuperMix-UDG (Invitrogen Life Technologies), respectively. The PCR primers and probes were obtained from Applied Biosystems. The primers used are *Nppa* Assay ID: Mm01255747_g1, *Nppb* Assay ID; Mm00435304_g1, *Col1a2* Assay ID; Mm01165187_m1, *Gapdh* Assay ID; 4352339E, *Il6* Assay ID; Mm99999064_m1, *Il1b* Assay ID; Mm01336189_m1, *Ifnb1* Assay ID; Mm00439546_s1 ,*Ifng* Assay ID; Mm99999071_m1, *Tnf* Assay ID; Mm00443260_g1, and *Dnase2a* Assay ID; Mm00438463_m1. We constructed quantitative PCR standard curves using the corresponding cDNA and all data were normalized to *Gapdh* mRNA content.

Europe PMC Funders Author Manuscripts

Histological Analysis

Heart samples were excised and immediately fixed in buffered 4% paraformaldehyde, embedded in paraffin, and cut into 5-μm thick sections. Hematoxylin and eosin or Azan-Mallory staining was performed on serial sections[5,23]. Myocyte cross-sectional area was measured by tracing the outline of 100 to 200 myocytes in each section[5,23]. For immunohistochemical analysis, frozen 5-μm thick heart sections were fixed in buffered 4% paraformaldehyde. The antibodies used were anti-mouse CD45 (ANASPEC), CD68 (Serotec), Ly6G/6C (BD Pharmingen), CD3 (Abcam), LAMP2a (Zymed), LC3[25], and TLR9 (Santa-Cruz). For *in situ* hybridization analysis, the mouse IL-6 (1-636) and IL-1β (1-810) RNA probes were labeled using DIG RNA Labeling Kit and detected using DIG Nucleic Acid Detection Kit (Roche Diagnostics). For immunoelectron microscopy, frozen heart tissue was embedded in the LR White resin and the deposited DNA was detected using anti-DNA antibody (Abcam) and immunogold conjugated anti-mouse IgG (British biocell International)[26]. For DNA detection, heart sections were incubated in PicoGreen (Molecular Probes) for 1 hour. We used EdU to detect mitochondrial DNA in the heart section. Twenty-four hours before TAC, mice were injected i.p. with 250 μg of EdU every 2 hours 5 times and EdU was detected using Click-iT EdU Alexa Fluor 488 Imaging Kit (Invitrogen).

In vitro and in vivo rescue experiments with the TLR9 inhibitor

Adult mouse cardiomyocytes were isolated from 12-14-week-old male mouse hearts as we previously described[5]. Cardiomyocytes were pre-treated with 1 μg/ml inhibitory CpG oligodeoxynucleotides (ODN2088) (Operon) (5′-tcctggcggggaagt-3′) or control oligodeoxynucleotides (ODN2088 control) (5′-tcctgagcttgaagt-3′) for 5 hours and incubated with 20 nM CCCP or 50 μM isoproterenol for 24 hours[20]. Cell death was estimated by Trypan blue staining[5]. To monitor mitochondrial $\Delta\Psi$, the cells were loaded with TMRE (Molecular Probe) at 10 nM for 30 minutes before observation. In *in vivo* study, the mice were injected i.v. with 500 μg of the oligodeoxynucleotides 2 hours before and 2 days after TAC, and mice were analyzed 4 days after TAC. To estimate survival, the mice received additional administration of the oligodeoxynucleotides 4 days after TAC and every 3 days thereafter.

Statistical analysis

Results are shown as the mean ± s.e.m. Paired data were evaluated using a Student's t-test. A 1-way ANOVA with the Bonferroni post hoc test was used for multiple comparisons. The Kaplan-Meier method with a Logrank test was used for survival analysis.

References

1. Mann DL. Inflammatory mediators and the failing heart: Past, present, and the foreseeable future. Circ Res. 2002; 91:988–998. [PubMed: 12456484]
2. Pollack Y, Kasir J, Shemer R, Metzger S, Szyf M. Methylation pattern of mouse mitochondrial DNA. Nucleic Acids Res. 1984; 12:4811–4824. [PubMed: 6330684]
3. Cardon L, Burge C, Clayton DA, Karlin S. Pervasive CpG suppression in animal mitochondrial genomes. Proc Natl Acad Sci U S A. 1994; 91:3799–3803. [PubMed: 8170990]
4. Gray MW, Burger G, Lang BF. Mitochondrial Evolution. Science. 1999; 283:1476–1481. [PubMed: 10066161]
5. Nakai A, et al. The role of autophagy in cardiomyocytes in the basal state and in response to hemodynamic stress. Nat Med. 2007; 13:619–624. [PubMed: 17450150]
6. Hemmi H, et al. A Toll-like receptor recognizes bacterial DNA. Nature. 2000; 408:740–745. [PubMed: 11130078]
7. Taanman J-W. The mitochondrial genome: structure, transcription, translation and replication. Biochim Biophys Acta - Bioenergetics. 1999; 1410:103–123.

8. Collins L, Hajizadeh S, Holme E, Jonsso n. I. Tarkowski A. Endogenously oxidized mitochondrial DNA induces in vivo and in vitro inflammatory responses. J Leukoc Biol. 2004; 75:995–1000. [PubMed: 14982943]
9. Mizushima N, Levine B, Cuervo AM, Klionsky DJ. Autophagy fights disease through cellular self-digestion. Nature. 2008; 451:1069–1075. [PubMed: 18305538]
10. Meerson F, Zaletayeva T, Lagutchev S, Pshennikova M. Structure and mass of mitochondria in the process of compensatory hyperfunction and hypertrophy of the heart. Exp Cell Res. 1964; 36:568–578. [PubMed: 14242242]
11. Bugger H, et al. Proteomic remodelling of mitochondrial oxidative pathways in pressure overload-induced heart failure. Cardiovascl Res. 2010; 85:376–384.
12. Evans CJ, Aguilera RJ. DNase II: genes, enzymes and function. Gene. 2003; 322:1–15. [PubMed: 14644493]
13. Kawane K, et al. Chronic polyarthritis caused by mammalian DNA that escapes from degradation in macrophages. Nature. 2006; 443:998–1002. [PubMed: 17066036]
14. Ashley N, Harris D, Poulton J. Detection of mitochondrial DNA depletion in living human cells using PicoGreen staining. Exp Cell Res. 2005; 303:432–446. [PubMed: 15652355]
15. Kabeya Y, et al. LC3, a mammalian homologue of yeast Apg8p, is localized in autophagosome membranes after processing. EMBO J. 2000; 19:5720–5728. [PubMed: 11060023]
16. Yamaguchi O, et al. Cardiac-specific disruption of the c-raf-1 gene induces cardiac dysfunction and apoptosis. J Clin Invest. 2004; 114:937–943. [PubMed: 15467832]
17. Lentz SI, et al. Mitochondrial DNA (mtDNA) biogenesis: Visualization and duel incorporation of BrdU and EdU into newly synthesized mtDNA in vitro. J Histochem Cytochem. 2010; 58:207–218. [PubMed: 19875847]
18. Takeuchi O, Akira S. Pattern recognition receptors and inflammation. Cell. 2010; 140:805–820. [PubMed: 20303872]
19. Zhang Q, et al. Circulating mitochondrial DAMPs cause inflammatory responses to injury. Nature. 2010; 464:104–107. [PubMed: 20203610]
20. Stunz L, et al. Inhibitory oligonucleotides specifically block effects of stimulatory CpG oligonucleotides in B cells. Eur J Immunol. 2002; 32:1212–1222. [PubMed: 11981808]
21. Bianchi ME. DAMPs, PAMPs and alarmins: all we need to know about danger. J Leukoc Biol. 2007; 81:1–5. [PubMed: 17032697]
22. Nakahira K, et al. Autophagy proteins regulate innate immune responses by inhibiting the release of mitochondrial DNA mediated by the NALP3 inflammasome. Nat Immunol. 2011; 12:222–230. [PubMed: 21151103]
23. Yamaguchi O, et al. Targeted deletion of apoptosis signal-regulating kinase 1 attenuates left ventricular remodeling. Proc Natl Acad Sci USA. 2003; 100:15883–15888. [PubMed: 14665690]
24. Koizumi T. Deoxyribonuclease II (DNase II) activity in mouse tissues and body fluids. Exp Anim. 1995:169–171. [PubMed: 7601228]
25. Lu Z, et al. Participation of autophagy in the degeneration process of rat hepatocytes after transplantation following prolonged cold preservation. Arch Histol Cytol. 2005; 68:71–80. [PubMed: 15827380]
26. Mosgoller W, et al. Distribution of DNA in human Sertoli cell nucleoli. J Histochem Cytochem. 1993; 41:1487–1493. [PubMed: 7504007]

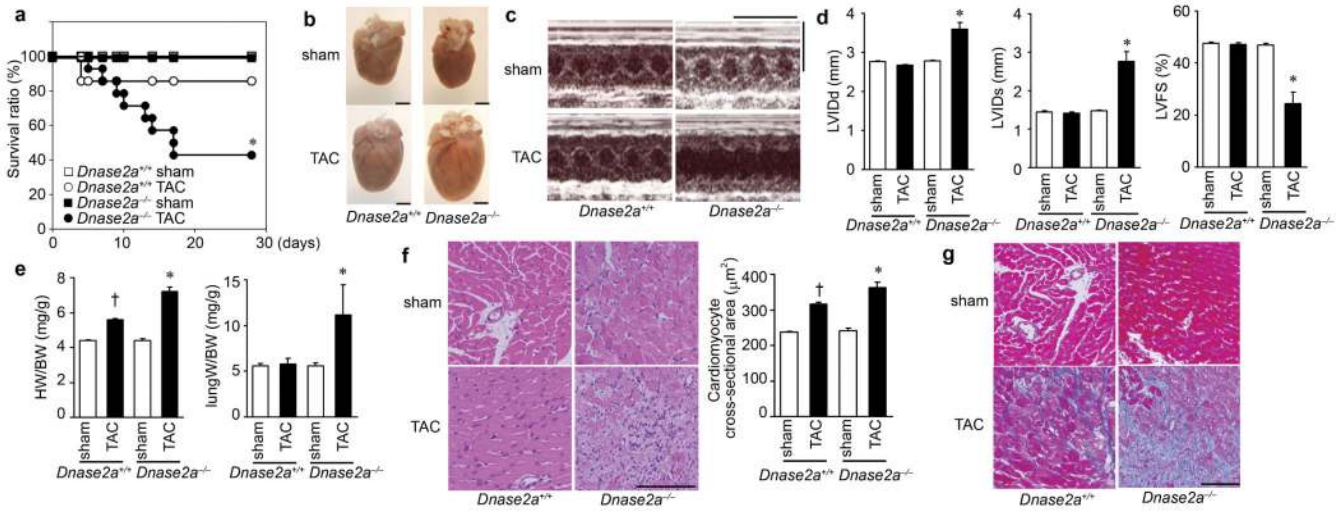

Fig. 1. TAC-induced cardiomyopathy in *Dnase2a*$^{-/-}$mice

a, Survival ratio after TAC ($n = 7 – 14$/group). **b** – **g**, 10 days after TAC. **b**, Gross appearance of hearts. Scale bar, 2 mm. **c**, Echocardiography. Scale bars, 0.2 sec and 5 mm. Echocardiographic (**d**) and physiological (**e**) parameters ($n = 7 – 13$/group). LVIDd and LVIDs indicate end-diastolic and end-systolic left ventricle (LV) internal dimension, respectively; LVFS, LV fractional shortening; HW/BW, heart/body weight. Hematoxylin-eosin-stained (**f**) and Azan-Mallory-stained (**g**) heart sections. Scale bar, 100 μm. Data are mean ± s.e.m. *$P < 0.05$ versus all other groups, †$P < 0.05$ versus sham-operated controls.

Europe PMC Funders Author Manuscripts

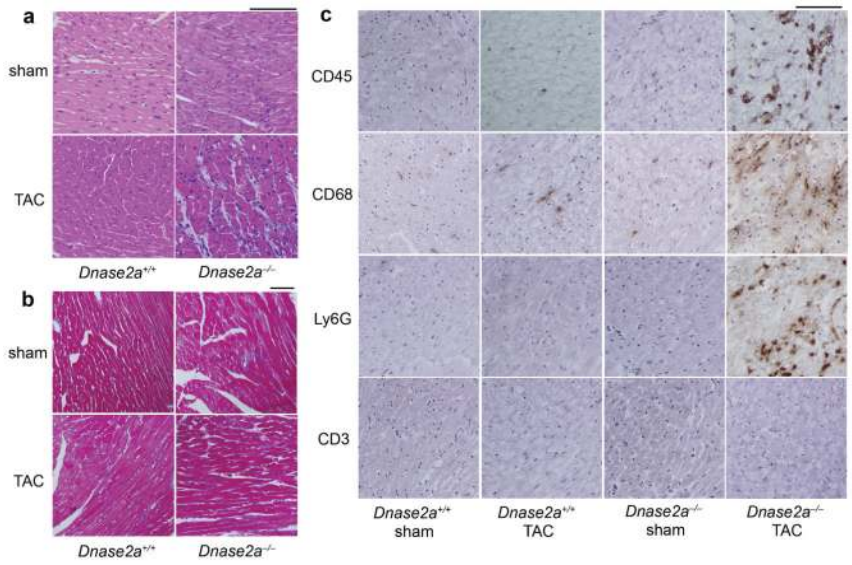

Fig. 2. Pressure overload-induced inflammatory responses in *Dnase2a*$^{-/-}$ mice 2 days after TAC

Mice are analyzed 2 days after TAC (**a** – **c**). **a**, Hematoxylin-eosin-stained heart sections. Scale bar, 100 μm. **b**, Azan-Mallory-stained sections. Scale bar, 100 μm. **c**, Immunohistochemical analysis using antibodies to CD45, CD68, Ly6G and CD3. Scale bar, 100 μm.

Europe PMC Funders Author Manuscripts

Europe PMC Funders Author Manuscripts

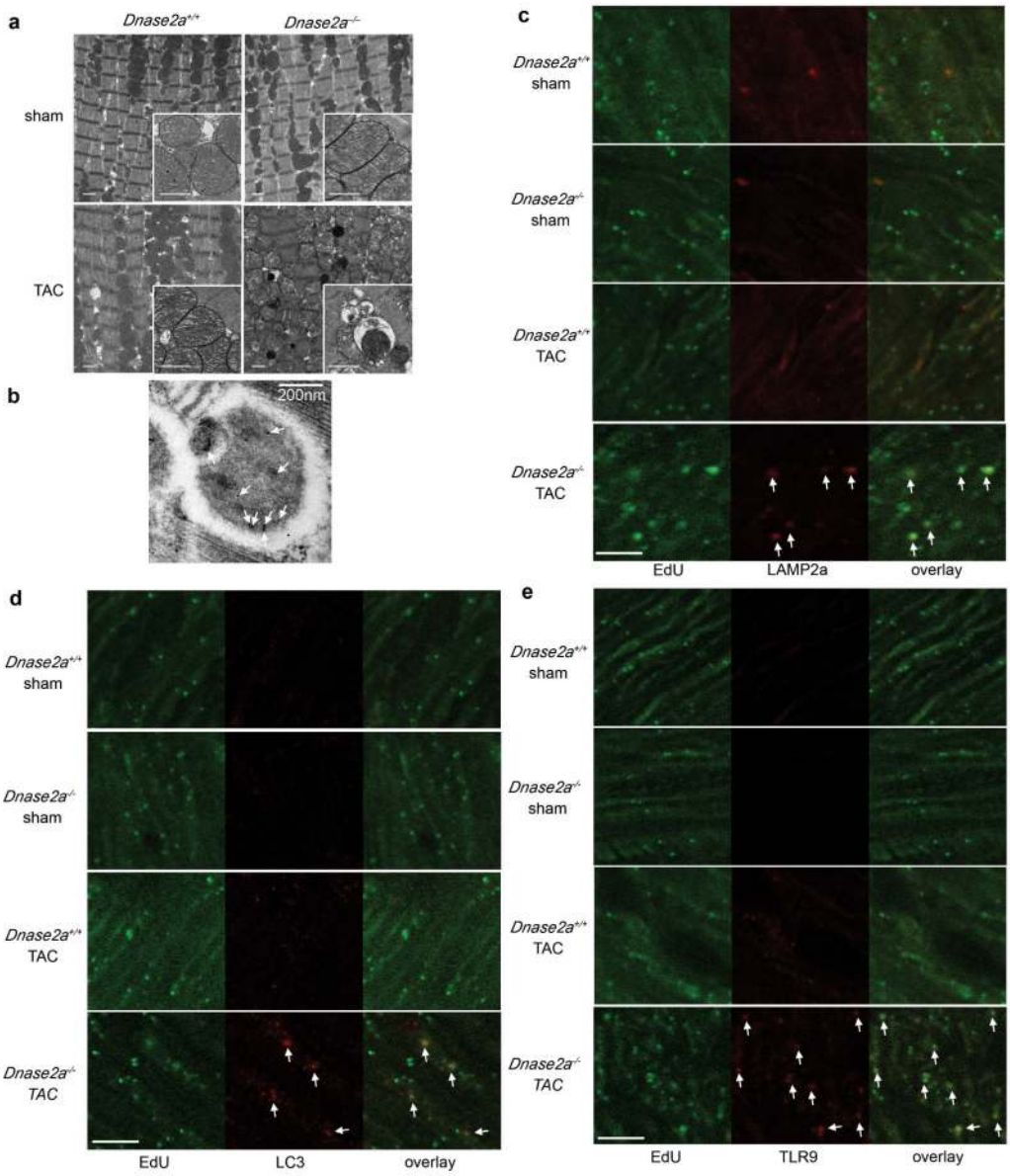

Fig. 3. Deposition of mitochondrial DNA in autolysosomes in pressure-overloaded *Dnase2a*$^{-/-}$ hearts

Mice were analyzed 2 days after TAC (**a**, **e**). **a**, Electron microscopic analysis. Images of mitochondria at higher magnification are shown in subsets. Scale bar, 1 μm. **b**, Autolysosome after incubation with anti-DNA antibody and 10 nm gold staining. Scale bar, 200 nm. Arrows indicate labeled DNA. Double staining of heart sections with EdU (green) and anti-LAMP2a antibody (red) (**c**), EdU (green) and anti-LC3 antibody (red) (**d**) or EdU and anti-TLR9 antibody (red) (**e**). Arrows indicate EdU-positive and LAMP2a-, LC3- or TLR9-positive structures. Scale bar, 10 μm.

Europe PMC Funders Author Manuscripts

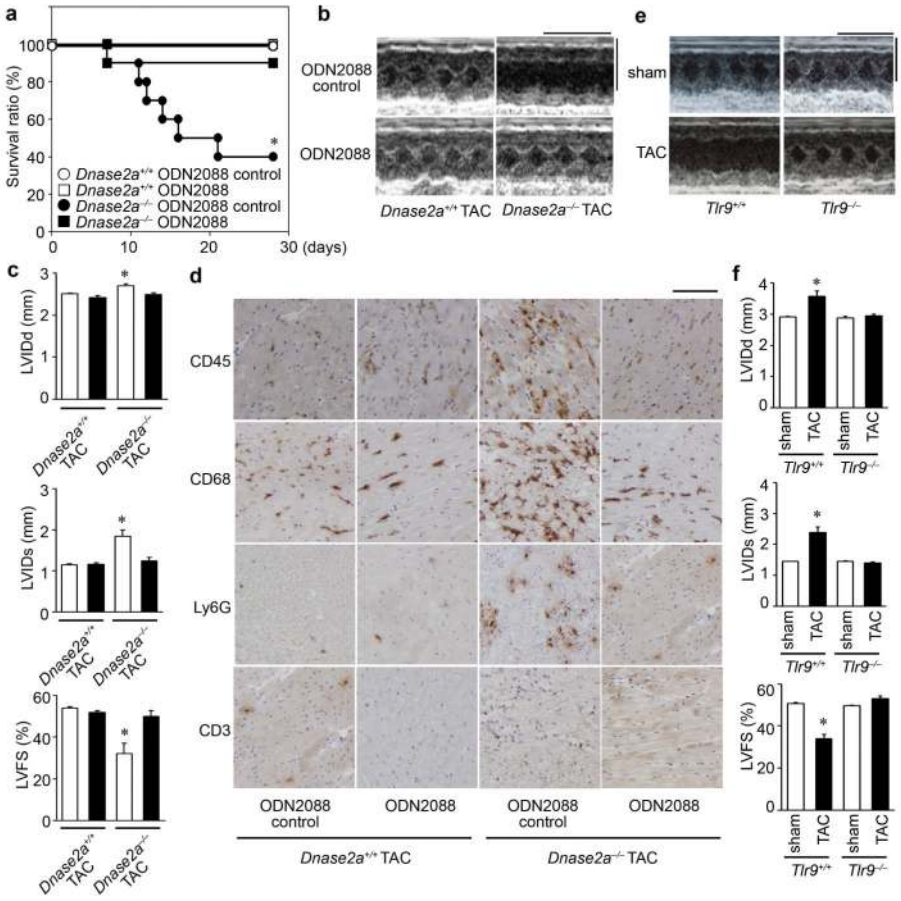

Fig. 4. Inhibition of TLR9 attenuated TAC-induced heart failure

a, Survival ratio of TAC-operated ODN-treated mice ($n = 6 – 10$/group). **b** - **d**, 4 days after TAC. **b**, Echocardiography. Scale bars, 0.2 sec and 5 mm. **c**, Echocardiographic parameters. Open and closed bars represent ODN2088 control- and ODN2088-treated groups, respectively ($n = 5 – 8$/group). **d**, Immunohistochemical analysis. Scale bar, 100 μm. TLR9-deficient mice were analyzed 10 weeks after TAC (**e**, **f**). **e**, Scale bars, 0.2 sec and 5 mm. **f**, Echocardiographic parameters ($n = 6 – 10$/group). Data are mean ± s.e.m. $*P < 0.05$ versus all other groups.